Comment on "Effect of viscous-convective subrange on passive scalar statistics at high Reynolds number"

Dhawal Buaria [1,2,*] and Katepalli R. Sreenivasan [1,3]
[1] *Tandon School of Engineering, New York University, New York, New York 11201, USA*
[2] *Max Planck Institute for Dynamics and Self-Organization, 37077 Göttingen, Germany*
[3] *Department of Physics and the Courant Institute of Mathematical Sciences, New York University, New York, New York 10012, USA*

(Received 28 July 2022; accepted 18 August 2023; published 5 September 2023)

Recently, Shete *et al.* [Phys. Rev. Fluids **7**, 024601 (2022)] explored the characteristics of passive scalars in the presence of a uniform mean gradient, mixed by stationary isotropic turbulence. They concluded that at high Reynolds and Schmidt numbers, the presence of both inertial-convective and viscous-convective ranges renders the statistics of the scalar and velocity fluctuations to behave similarly. However, their data included Schmidt numbers of 0.1, 0.7, 1.0, and 7.0, only the last of which can (at best) be regarded as moderately high. Additionally, they do not consider already available data in the literature at substantially higher Schmidt number of up to 512. By including these data, we demonstrate here that the differences between velocity and scalar statistics show no vanishing trends with increasing Reynolds and Schmidt numbers, and essential differences remain intact at all Reynolds and Schmidt numbers.

DOI: 10.1103/PhysRevFluids.8.097601

I. INTRODUCTION

In Ref. [1], Shete *et al.* investigate the mixing of a passive scalar $\theta(\mathbf{x}, t)$ in isotropic turbulence, driven by a uniform mean gradient $\nabla\Theta = (G, 0, 0)$:

$$\partial\theta/\partial t + \mathbf{u}\cdot\nabla\theta = -\mathbf{u}\cdot\nabla\Theta + D\nabla^2\theta, \tag{1}$$

where D is the scalar diffusivity and $\mathbf{u}(\mathbf{x}, t)$ is the underlying turbulent velocity field governed by the incompressible Navier-Stokes equations. The mixing characteristics are governed by two parameters: the Schmidt number $\mathrm{Sc} = \nu/D$, ν being the kinematic viscosity of the fluid and the Taylor-scale Reynolds number $\mathrm{Re}_\lambda = u'\lambda/\nu$, where u' is the root-mean-square velocity fluctuation and λ is the Taylor length scale. The data of Ref. [1], obtained from state-of-the-art direct numerical simulations (DNS), correspond to $\mathrm{Re}_\lambda = 633$ and $\mathrm{Sc} = 0.1, 0.7, 1.0, 7.0$. The Reynolds number is high enough to display inertial range characteristics, but the Schmidt number range is very limited. Given that turbulent mixing for $\mathrm{Sc} > 1$ is fundamentally different from that for $\mathrm{Sc} < 1$, the authors essentially have a single data point at $\mathrm{Sc} = 7$ in the $\mathrm{Sc} > 1$ regime, making their inferences unsound. Further, the authors did not include the data already available in the literature at much higher

*dhawal.buaria@nyu.edu

Schmidt numbers. Here, we include them as well and demonstrate that the conclusions in [1] are not correct and need to be revised.

The analysis in Ref. [1] is built around the following three points: (i) the skewness of scalar gradients; (ii) a comparison of the intermittency exponent of scalar dissipation rate to that of energy dissipation rate; and (iii) a comparison between the probability density functions (PDFs) of scalar and energy dissipation rates. Note that for an eddy of characteristic size r, inertial and inertial-convective ranges are both defined by the condition $\eta_K \ll r \ll L$, where η_K is the Kolmogorov length scale, marking the viscous cutoff, and L is the large scale at which the energy is injected; the viscous convective range is defined by $\eta_B \ll r \ll \eta_K$, where $\eta_B = \eta_K \mathrm{Sc}^{-1/2}$ is the Batchelor length scale. Evidently, a fully developed viscous convective range requires $\mathrm{Sc} \gg 1$ (and unlikely to exist at $\mathrm{Sc} = 7$). Here, we assess each of the three points above and show that fundamental differences remain between velocity and scalar statistics even at high Sc, essentially demonstrating—contrary to the conclusion of Ref. [1]—that velocity and scalar statistics are never similar.

II. ANISOTROPY OF SCALAR GRADIENTS

It is now well known that local isotropy is violated for a passive scalar driven by a uniform mean gradient [2–4]. Specifically, for the scalar gradient in the direction of the imposed mean gradient, $\nabla_\parallel \theta$, the odd moments are nonzero of the order unity (whereas local isotropy requires them to be zero). This violation of local isotropy can be traced to the existence of so-called ramp-cliff structures [2,4,5], resulting from a direct influence of the imposed large-scale mean gradient on the small-scale scalar field.[1] Based on the specific ramp-cliff model of Ref. [4], Shete *et al.* reported the following expression (Eq. (10) of Ref. [1]):

$$\frac{\langle (\nabla_\parallel \theta)^p \rangle}{\langle (\nabla_\parallel \theta)^2 \rangle^{p/2}} \sim \mathrm{Sc}^{-1/2} \mathrm{Re}_\lambda^{(p-3)/2}, \qquad p = 3, 5, 7 \dots, \tag{2}$$

which quantifies the scaling of odd-moments of $\nabla_\parallel \theta$. Using only two data points for $\mathrm{Sc} = 1, 7$ and restricting the testing for $p = 3$ (see Fig. 7 of Ref. [1]), the authors concluded that Eq. (2) is valid.

We first note that the result in Eq. (2), implicitly given in Ref. [4], was explicitly derived in [5], which Shete *et al.* did not recognize. Additionally, the authors also ignore that Eq. (2), along with the underlying assumptions, was rigorously tested in Ref. [5] by using DNS data over a large range of Schmidt numbers $\mathrm{Sc} = 1 - 512$ (at $\mathrm{Re}_\lambda = 140$) and also for moment orders $p = 3$, 5 and 7. Comprehensive details about the DNS and numerical methods are available in Refs. [6–8], whereas the database along with simulation parameters is outlined in Refs. [5,9]. In Ref. [5], it was found that the original ramp-cliff model required modifications and the scaling of odd moments of $\nabla_\parallel \theta$ is better described by the following expression:

$$\frac{\langle (\nabla_\parallel \theta)^p \rangle}{\langle (\nabla_\parallel \theta)^2 \rangle^{p/2}} \sim \mathrm{Sc}^{-1/2+\alpha}\, \mathrm{Re}_\lambda^{(p-3)/2}, \qquad \text{for } p = 3, 5, 7 \dots . \tag{3}$$

where the new exponent on Sc, with $\alpha \approx 0.05$, represents a slightly weaker slope compared to $-1/2$ in Eq. (2). As shown in Ref. [5], this implies that a new scale $\eta_D = \eta_B \mathrm{Sc}^\alpha$ ($\alpha \approx 0.05$) marks the true diffusive cutoff scale in the scalar field (instead of η_B). The difference between η_B and η_D arises because the scalar dissipation anomaly does not hold for large Sc [9–11]. A similar idea was also proposed in an independent study [12].

A reinspection of Fig. 7 of Ref. [1] shows that the data for $\mathrm{Sc} = 1, 7$ noticeably depart from the $\mathrm{Sc}^{-1/2}$ scaling but are consistent with the updated result in Eq. (3). For completeness, we combine the data for $p = 3$ for various Re_λ and Sc in Fig. 1 (including previously unreported data at $\mathrm{Re}_\lambda = 390$, which is also large enough for inertial-range scaling to exist [9]). Evidently, the data at $\mathrm{Re}_\lambda =$

[1] In fact, even in absence of a large-scale mean gradient, similar structures are observed in the scalar field [27].

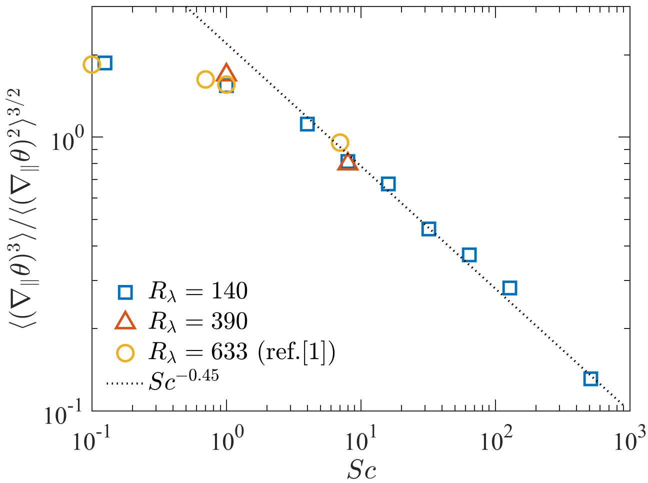

FIG. 1. Skewness of $\nabla_{\|}\theta$ as a function of Sc, for various Re_λ. The data for $\mathrm{Re}_\lambda = 390$ and 633 are, respectively, adjusted by factors 1. 2, and 0.9 to account for a very weak Re_λ dependence, but do not have any bearing on trends with Sc.

140 are consistent with modified Sc scaling in Eq. (3) (with $\alpha = 0.05$). Data at higher Re_λ are also in agreement with the trends at $\mathrm{Re}_\lambda = 140$, though significantly higher Sc would be required to see if α has a Re_λ dependence. However, Shete *et al.* did not examine the results for $p = 5, 7$, nor tested the veracity of the length scale η_D, both of which are especially important given the lack of high-Sc data in their work.

Notwithstanding the quantitative differences, it is clear that the odd moments decrease as Sc increases, presumably approaching zero, i.e., local isotropy is restored at infinite Sc. Shete *et al.* invoked this notion to conclude that due to increased scale separation at high Re_λ and Sc, the scalar statistics become universal and hence similar to velocity statistics. This conclusion is unjustified because even though local isotropy of the scalar is restored at $\mathrm{Sc} \to \infty$, scalar dissipation anomaly is also simultaneously violated [9], while the dissipation anomaly for energy dissipation rate continues to hold. This is a fundamental difference between velocity and scalar statistics, which implies that they can never be similar at any Re_λ and Sc. Shete *et al.* assume that scalar dissipation anomaly is valid based on just two data points $\mathrm{Sc} = 1, 7$, but also note that this assumption would not hold at higher Sc (implying that their assumption and conclusions are contradictory).

III. INTERMITTENCY EXPONENT OF SCALAR AND VELOCITY GRADIENTS

With respect to the second point, Shete *et al.* investigated the intermittency of local averages (over scale r) of energy dissipation ϵ_r and scalar dissipation χ_r. Following Kolmogorov's refined hypothesis [13], it is expected that:

$$\langle\epsilon_r^2\rangle \sim r^{-\mu}, \quad \langle\chi_r^2\rangle \sim r^{-\mu_\theta}, \tag{4}$$

for r in the inertial range (and the inertial-convective range for the scalar). Here, μ is the well-known intermittency exponent for the energy dissipation and μ_θ for the scalar dissipation. Previous studies have shown that $\mu \approx 0.25$ and $\mu_\theta \approx 0.35$ for scalars corresponding to $\mathrm{Sc} \sim 1$ [14–16]. In Fig. 8 of Ref. [1], Shete *et al.* extract the intermittency exponents using some approximations and find that, indeed, $\mu \approx 0.25$, and $\mu_\theta > \mu$ for $\mathrm{Sc} \leqslant 1$, in essential agreement with previous studies [14–16]. Additionally, they infer that μ_θ decreases to 0.25 when $\mathrm{Sc} = 7$, and conclude once again that velocity and scalar statistics are similar at high Sc.

However, this conclusion is erroneous because the authors simply captured the slight decline of μ_θ at one Sc. Indeed, had they used data from larger Sc, it would have been clear that the scalar intermittency exponents μ_θ does not stay matched with μ for large Sc, but monotonically decreases, seemingly to zero as Sc $\to \infty$; see Fig. 5 of Ref. [17]. Such an approach to zero is consistent with the violation of scalar dissipation anomaly at infinite Sc. Since $\mu_\theta > \mu$ at Sc $= 1$ and $\mu_\theta \to 0$ at Sc $\to \infty$, it naturally follows that $\mu_\theta = \mu$ at some intermediate Sc, which is precisely what Shete *et al.* find for Sc $= 7$. But this does not imply that velocity and scalar statistics become similar at high Sc.

IV. PDF OF SCALAR AND ENERGY DISSIPATION

For the third point, Shete *et al.* consider the PDFs of energy dissipation rate ϵ and scalar dissipation rate χ. Based on their Fig. 9, they conclude that as Sc increases, the PDFs of χ and ϵ approach each other. First, it can be clearly seen from their Fig. 9 that the two PDFs do not coincide: the discrepancy may appear to be small because the plot shows the PDFs of logarithms of ϵ and χ. The differences between the PDFs of ϵ and χ would be far more conspicuous. Furthermore, it is well known that PDFs of highly intermittent quantities, such as ϵ and χ for Sc ~ 1 are close to log normal. Thus, it is not a surprise that all the PDFs shown in Fig. 9 of Ref. [1] are close to each other. However, with much higher range of Sc (albeit at lower Re_λ), it has been demonstrated previously [18] that PDF of χ becomes increasingly different from that of ϵ as Sc increases. Thus the behavior observed by Shete *et al.* in Fig. 9 is also just transitory for one Sc.

It is worth mentioning that, for both the intermittency exponent and PDF, Shete *et al.* utilize the energy dissipation to represent small-scale velocity field. However, energy dissipation is not the only measure of velocity gradients statistics. Other measures, such as the enstrophy Ω are equally viable. In this regard, it is well known that Ω is more intermittent than ϵ; for instance, the intermittency exponent of Ω is larger than that of ϵ [17,19]. Moreover, the two PDFs are distinctly different from each other, even at very high Reynolds numbers [20,21]. Additionally, there are numerous other distinct differences between the fine scale structure of scalar and velocity gradients, especially considering the latter are strongly influenced by the nonlocal pressure field [22–25]. Thus, simply comparing scalar dissipation with energy dissipation does not attest to the similarity of scalar and velocity statistics.

V. VELOCITY AND SCALAR STRUCTURE FUNCTIONS

In addition to the above three points, we consider an additional argument, which was not considered by Shete *et al.*, but clearly negates their conclusion. The differences between velocity and scalar fields can also be demonstrated by comparing their respective structure functions. If we represent the velocity and scalar increments over scale r by $\delta_r u$ and $\delta_r\theta$, respectively, then in the inertial range, the pth-order structure functions are expected to follow the power laws:

$$\langle(\delta_r u)^p\rangle \sim r^{\zeta_p}, \quad \text{and} \quad \langle(\delta_r\theta)^p\rangle \sim r^{\xi_p}. \tag{5}$$

If the velocity and scalar statistics are indeed similar at high Re_λ and Sc, we should obtain $\zeta_p = \xi_p$. Note, $\zeta_p = \xi_p = p/3$ for the K41 phenomenology, but it is well known that both exponents strongly depart from K41 due to intermittency, with scalar exponents ξ_p departing more strongly [3,26]. While previous studies were mostly restricted to Sc ~ 1, the effect of increasing Sc was more recently studied in Ref. [9]; where it was found that with increasing Sc, the deviation of ξ_p from the K41 result is even stronger. In the limit of Sc $\to \infty$, it was observed that ξ_p behave similar to Burgers' turbulence [9]. Essentially, the discrepancy between ζ_p and ξ_p increases with Sc; again demonstrating that velocity and scalar statistics cannot be similar.

VI. SUMMARY AND CONCLUSION

To summarize, by considering the entire data available, we have demonstrated that the velocity and scalar fields depart increasingly from each other as the Schmidt number increases. This is not a surprising conclusion but seems important to set right in view of the erroneous conclusion of Ref. [1], based on simulations at just one value of Sc > 1.

[1] K. P. Shete, D. J. Boucher, J. J. Riley, and S. M. de Bruyn Kops, Effect of viscous-convective subrange on passive scalar statistics at high reynolds number, Phys. Rev. Fluids **7**, 024601 (2022).
[2] K. R. Sreenivasan, R. A. Antonia, and D. Britz, Local isotropy and large structures in a heated turbulent jet, J. Fluid Mech. **94**, 745 (1979).
[3] Z. Warhaft, Passive scalars in turbulent flows, Annu. Rev. Fluid Mech. **32**, 203 (2000).
[4] K. R. Sreenivasan, Turbulent mixing: A perspective, Proc. Natl. Acad. Sci. **116**, 18175 (2019).
[5] D. Buaria, M. P. Clay, K. R. Sreenivasan, and P. K. Yeung, Small-Scale Isotropy and Ramp-Cliff Structures in Scalar Turbulence, Phys. Rev. Lett. **126**, 034504 (2021).
[6] M. P. Clay, D. Buaria, T. Gotoh, and P. K. Yeung, A dual communicator and dual grid-resolution algorithm for petascale simulations of turbulent mixing at high Schmidt number, Comput. Phys. Commun. **219**, 313 (2017).
[7] M. P. Clay, D. Buaria, P. K. Yeung, and T. Gotoh, GPU acceleration of a petascale application for turbulent mixing at high Schmidt number using OpenMP 4.5, Comput. Phys. Commun. **228**, 100 (2018).
[8] M. P. Clay, D. Buaria, and P. K. Yeung, Improving scalability and accelerating petascale turbulence simulation using OpenMP, in *Proceedings of OpenMP Conference* (Stony Brook University, 2017).
[9] D. Buaria, M. P. Clay, K. R. Sreenivasan, and P. K. Yeung, Turbulence is an Ineffective Mixer when Schmidt Numbers Are Large, Phys. Rev. Lett. **126**, 074501 (2021).
[10] M. S. Borgas, B. L. Sawford, S. Xu, D. A. Donzis, and P. K. Yeung, High Schmidt number scalars in turbulence: Structure functions and Lagrangian theory, Phys. Fluids **16**, 3888 (2004).
[11] D. Buaria, P. K. Yeung, and B. L. Sawford, A Lagrangian study of turbulent mixing: Forward and backward dispersion of molecular trajectories in isotropic turbulence, J. Fluid Mech. **799**, 352 (2016).
[12] T. Yasuda, T. Gotoh, T. Watanabe, and I. Saito, Péclet-number dependence of small-scale anisotropy of passive scalar fluctuations under a uniform mean gradient in isotropic turbulence, J. Fluid Mech. **898**, A4 (2020).
[13] A. N. Kolmogorov, A refinement of previous hypotheses concerning the local structure of turbulence in a viscous incompressible fluid at high Reynolds number, J. Fluid Mech. **13**, 82 (1962).
[14] R. R. Prasad, C. Meneveau, and K. R. Sreenivasan, Multifractal Nature of the Dissipation Field of Passive Scalars in Fully Turbulent Flows, Phys. Rev. Lett. **61**, 74 (1988).
[15] K. R. Sreenivasan and P. Kailasnath, An update on the intermittency exponent in turbulence, Phys. Fluids A: Fluid Dyn. **5**, 512 (1993).
[16] L. Mydlarski and Z. Warhaft, Passive scalar statistics in high-Péclet-number grid turbulence, J. Fluid Mech. **358**, 135 (1998).
[17] D. Buaria and K. R. Sreenivasan, Intermittency of turbulent velocity and scalar fields using three-dimensional local averaging, Phys. Rev. Fluids **7**, L072601 (2022).
[18] J. Schumacher, K. R Sreenivasan, and P. K. Yeung, Very fine structures in scalar mixing, J. Fluid Mech. **531**, 113 (2005).
[19] S. Chen, K. R. Sreenivasan, and M. Nelkin, Inertial Range Scalings of Dissipation and Enstrophy in Isotropic Turbulence, Phys. Rev. Lett. **79**, 1253 (1997).
[20] D. Buaria, A. Pumir, E. Bodenschatz, and P. K. Yeung, Extreme velocity gradients in turbulent flows, New J. Phys. **21**, 043004 (2019).
[21] D. Buaria and A. Pumir, Vorticity-Strain Rate Dynamics and the Smallest Scales of Turbulence, Phys. Rev. Lett. **128**, 094501 (2022).

[22] W. T. Ashurst, A. R. Kerstein, R. M. Kerr, and C. H. Gibson, Alignment of vorticity and scalar gradient with strain rate in simulated Navier-Stokes turbulence, Phys. Fluids **30**, 2343 (1987).

[23] D. Buaria, E. Bodenschatz, and A. Pumir, Vortex stretching and enstrophy production in high Reynolds number turbulence, Phys. Rev. Fluids **5**, 104602 (2020).

[24] A. Garcia and M. Gonzalez Analysis of passive scalar gradient alignment in a simplified three-dimensional case, Phys. Fluids **18**, 058101 (2006).

[25] D. Buaria, A. Pumir, and E. Bodenschatz, Generation of intense dissipation in high Reynolds number turbulence, Philos. Trans. R. Soc. A **380**, 20210088 (2022).

[26] K. R. Sreenivasan and R. A. Antonia, The phenomenology of small-scale turbulence, Annu. Rev. Fluid Mech. **29**, 435 (1997).

[27] T. Watanabe and T. Gotoh, Statistics of a passive scalar in homogeneous turbulence, New J. Phys. **6**, 40 (2004).